

Probing the anomalous positron fraction origin with fully leptonic decaying gravitino dark matter candidates

Johannes Buchner,^{a,b} Edson Carquin,^d Marco A. Díaz,^c
Germán A. Gómez-Vargas,^{1a} Boris Panes,^a Nicolás Viaux^d

^aInstituto de Astrofísica, Pontificia Universidad Católica de Chile, Avenida Vicuña Mackenna 4860, Santiago, Chile

^bMillenium Institute of Astrophysics, Vicuña MacKenna 4860, 7820436 Macul, Santiago, Chile

^cInstituto de Física, Pontificia Universidad Católica de Chile, Avenida Vicuña Mackenna 4860, Santiago, Chile

^dDepartamento de Física y Centro Científico- Tecnológico de Valparaíso (CCTVal), Universidad Técnica Federico Santa María, Av. España 1680, Valparaíso, Chile

E-mail: johannes.buchner.acad@gmx.com, edson.carquin@usm.cl,
mad@susy.fis.puc.cl, ggomezv@uc.cl, bpanes@astro.puc.cl, nicolas.viaux@usm.cl

Abstract. The flux of electron and positron cosmic rays measured by the space-based experiments PAMELA, AMS-02, CALET, DAMPE and Fermi-LAT shows an unexpected behaviour at high energies, in comparison with expectations from standard astrophysical sources. In particular, AMS-02 observations provide compelling evidence for a new source of positrons and electrons whose origin is still unknown. Plausible scenarios include either the contribution of dark matter or unresolved astrophysical sources, such as nearby pulsars. It has been shown that explanations based mostly on dark matter, tend to overproduce γ -rays, entering in conflict with measurements of the extra-galactic γ -ray background (EGB). Although this situation seems to be quite generic, it ultimately depends on the properties of the dark matter candidate. In this work we revisit a model in which the gravitino is a dark matter candidate decaying to SM particles through R-parity violating couplings. We show that decay channels allowed by trilinear couplings produce more electrons and positrons and fewer photons in comparison to channels allowed by bilinear couplings. Indeed, when considering AMS-02 data alone we find that the trilinear model is compatible with EGB constraints. However, this result may change when DAMPE or CALET measurements of the sum of electrons and positrons fluxes are considered instead of AMS-02 data. Therefore, in order to evaluate this model further, discrepancies between the data collected by these experiments need to be clarified.

Keywords: dark matter experiments, cosmic ray experiments, gamma ray experiments, dark matter theory

¹Now Corporate Data Scientist at [Derco](#),

1 Introduction

The energy spectrum of electrons and positrons measured by experiments such as PAMELA [1], AMS-02 [2–4], CALET [5], DAMPE [6] and Fermi-LAT [7] show noticeable discrepancies when compared to predictions based on standard astrophysical sources, such as cosmic-ray interactions or emissions from pulsars. These experimental signals suggest that extra sources of (primary) positrons are required in order to make sense of the data.

It is well known that an extra source of cosmic rays can be obtained from Dark Matter (DM) annihilations or decays [8]. For instance, it has been shown that the anomalous measurement of positrons, initially reported by PAMELA [1] and later confirmed by AMS-02 [2], can be well explained by considering a distribution of DM particles that can annihilate or decay to charged leptons both as primary or secondary particles [9–14]. This generic picture, however, when looking at the produced gamma ray spectrum, becomes in conflict with the measurement of the extra galactic gamma-ray background (EGB) derived from Fermi-LAT [7]. As an example about this issue, we refer to our previous work [15], where we test a DM scenario that contains a gravitino as the lightest super-symmetric particle (LSP) and bilinear R-parity violation (BRpV) couplings [16]. We found that this model is able to describe the anomalous positron fraction measured by AMS-02, but at the cost of producing a flux of γ -rays overshooting the EGB limits.

In this work, we continue with the study of gravitino models, basically searching for scenarios where the production of γ -rays could be reduced to stay away from the EGB constraint. In particular, we suggest that this can be achieved by moving from BRpV to trilinear R-parity violating (TRpV) couplings, since the tree-level gravitino decay modes allowed in each scenario are completely different. For instance, in TRpV the gravitino is allowed to decay to two charged leptons plus a neutrino, such as $\psi \rightarrow l^\mp l^\pm \nu$ with $l = e, \mu, \tau$, while in BRpV the gravitino decays involve two-body decays including leptons and higgs/gauge bosons, such as $\psi \rightarrow l^\mp W^\pm$ and $\psi \rightarrow \nu H/Z$. In practice, we have noticed that preferred three-body decays, which are useful to fit the positron data, produce more charged leptons than two-body decays for the same lifetime, which is helpful to reduce the associated emission of gamma-rays. Although this approach seems to work for the analysis of AMS-02 and the EGB, we notice that the data reported from CALET and DAMPE may have a relevant impact on this conclusion.

The paper is organized as follows. In section 2 we describe the decaying gravitino DM model with R-Parity violating couplings. In section 3 we compare trilinear and bilinear decay channels in order to show the features of TRpV that allow a better comparison to cosmic ray data. In section 4 we define the relevant contributions to the electron, positron and photon flux. In section 6 we discuss the data considered in the current analysis and the statistical tests of our model. In section 7 we comment on these findings. Finally, in section 8 we summarize our conclusions and perspectives.

2 Dark Matter model

We consider a super-symmetric (SUSY) extension of the standard model (SM) with a low energy spectrum characterized by a gravitino as the lightest SUSY particle (LSP), that can decay to final state leptons through R-Parity violating couplings [16, 17]. In this scenario, the decay of the gravitino LSP can be achieved in two steps.

First, we consider R-Parity conserved interactions between the gravitino, one SM fermion and the corresponding scalar super-partner, which in principle do not allow the direct decay

of the gravitino. If we represent the SM fermions by ψ , the scalar super-partners as ϕ and the gravitino field as Ψ_μ , we can write the Lagrangian associated to this interaction as:

$$\mathcal{L} = -\frac{1}{\sqrt{2}M_*}\bar{\psi}_L\gamma^\mu\gamma^\nu\partial_\nu\phi\Psi_{\mu R} \quad (2.1)$$

where the L/R indices standing for left/right chirality, γ^μ being the Dirac matrices and $M_* = (8\pi GN)^{-1/2} = 2.4 \times 10^{18}$ GeV the reduced Planck mass. In this notation the mass of the gravitino is given by $m_G = F/\sqrt{3}M_*$, with F the scale of spontaneous-SUSY breaking.

Second, we must consider R-Parity violating interactions, which in practice allow the decay of one single superpartner into final state channels that only contain SM particles. These interactions are modelled by the following superpotential,

$$W_{\mathcal{RP}} = \frac{1}{2}\lambda_{ijk}L_iL_jE_k^c + \lambda'_{ijk}L_iQ_jD_k^c + \lambda''_{ijk}U_iD_jD_k^c + \epsilon_i H L_i, \quad (2.2)$$

which is written in terms of superfields and scalar couplings. This superpotential includes left-handed lepton and quarks superfields (L) and (Q), the up-type Higgs superfield (H), right-handed lepton and quark superfields (E^c) and (U^c, D^c). The indices i, j, k run over flavor generations, $\lambda_{ijk}, \lambda'_{ijk}, \lambda''_{ijk}$ are dimensionless coupling constants and ϵ_i are dimension one parameters.

The bilinear term of Eq. 2.2, controlled by the coupling ϵ_i , determines the strength of two body gravitino decays, such as $\psi \rightarrow H\nu, W^\pm l^\mp, Z\nu$. In a previous work [15] we have considered these decays in order to adjust the AMS-02 positron anomaly, but we have also found that the model is in tension with EGB limits from Fermi-LAT. Here we consider these results in order to guide the search of viable scenarios. In particular, we focus on the first type of interactions, which are controlled by the couplings λ_{ijk} , since these terms allow the three-body decay of gravitinos to pairs of opposite charged leptons plus one neutrino, such as $\psi \rightarrow l_i^- l_j^+ \nu_k$. We consider only these terms because the decay channels contain charged leptons, which are useful to adjust the positron anomaly, but also because we can get lower amounts of γ radiations in comparison to the cases where we have quarks as final states, which appear when λ'_{ijk} and λ''_{ijk} are switched on. In [17], we can find the analytical expressions for the decay rates for every combination of leptons produced by λ_{ijk} terms. In Appendix A, we also discuss the possibility to use only these terms of the superpotential to explain at least one of the neutrino masses, such as in reference [18]. We notice that the heavy mass of the scalars, which is required to make the lifetime of the gravitino sufficiently small, also allow neutrino mass contributions considering reasonable values of trilinear couplings.

3 Comparison between BRpV and TRpV scenarios

When we consider a SUSY model that includes BRpV terms [16], it is possible to have tree-level interactions between a gravitino and two SM particles. Thus, for a gravitino mass above the TeV scale, which is necessary to adjust the positron anomaly [3], gravitinos can decay through on-shell two-body final state channels, that can contain gauge bosons and leptons ($\psi \rightarrow Z\nu$ and $\psi \rightarrow W^\pm l^\mp$) or a Higgs particle plus neutrinos ($\psi \rightarrow H\nu$). In particular, in our previous work [15], we have shown that the preferred gravitino lifetime in this case is $1.0 (1.3) \times 10^{26}$ s for $m_G = 1 (2)$ TeV. The preferred channel is mostly given by $\psi \rightarrow W^\pm \tau^\mp$, with 90% (80%) of the total branching fraction.

Instead, when we consider TRpV interactions [16], it is possible to have tree-level interactions between the gravitino, one SUSY scalar particle and the corresponding SM fermion,

which can be obtained from the first term of Eq. 2.2. Thus, when scalars are considered to be super heavy, such as in Split-SUSY models [19] or in order to enhance the gravitino lifetime (Appendix A), gravitinos only can decay through off-shell three-body final state channels, which in general include two charged leptons plus a neutrino ($\psi \rightarrow l^\mp l^\pm \nu$). Notice that the branching fractions of conjugated channels must be equal, such that $Br(\psi \rightarrow l'^\mp l^\pm \nu) = Br(\psi \rightarrow l'^\pm l^\mp \nu)$.

Now let us discuss some features that arise when we consider the predicted spectrum of charged leptons in TRpV models. For simplicity, we focus on the measurement of electrons, but the positron case is analogous and symmetric. In this case we can consider that neutrino flavors are indistinguishable, thus in principle we only have to deal with nine channels, which we can list from 1 to 9 as $\psi \rightarrow l_i^- l_j^+ \nu$ with $i, j = e, \mu, \tau$. We must notice that the electron spectrum of each element of the group $l'^- l^+ \nu$ with l' fixed, generates a very similar spectra, which is shown in Fig. (1) right panel. This feature allows us to reduce the number of effective independent channels to adjust the electron-positron data from nine to three. In section 6 we use this feature to show that the preferred gravitino lifetime in this case is $4.6 (3.6) \times 10^{26} \text{ s}$ for $m_G = 1.3 (2.3) \text{ TeV}$. The preferred channel is mostly given by $\psi \rightarrow \tau^- l_i^+ \nu$ with $i = e, \mu, \tau$, with 54% (58%) of the total branching fraction.

From these results we can see that in TRpV we requires a gravitino lifetime ($3.6 \times 10^{26} \text{ s}$) which is slightly larger than the one obtained in BRpV ($1.3 \times 10^{26} \text{ s}$). This is because the preferred channel in TRpV ($\tau^- l^+ \nu$) generates relatively more electrons than the preferred channel in BRpV ($W^+ \tau^-$), which can be checked by comparing the red curves in both plots of Fig. (1). This effect is probably due to phase space differences between three-body and two-body decays, which may be interesting to understand further. However, in this work we consider that the visual inspection of the spectra behavior is enough to motivate a further study of the TRpV scenario.

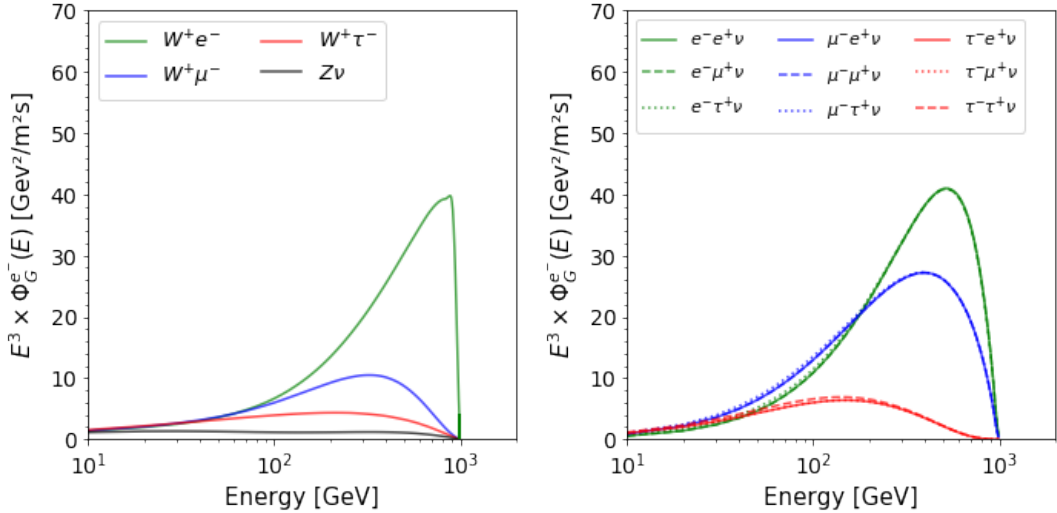


Figure 1. Electron spectrum of bilinear (left panel) and trilinear (right panel) decay channels. In both cases we consider those channels that are able to produce prompt electrons. The gravitino lifetime is the same and equal to $\tau_G = 10^{26} \text{ s}$ in both panels.

Furthermore, we also can check that, for the same gravitino lifetime, the gamma-ray

spectra produced by BRpV channel ($W^+\tau^-$) generates a slightly higher photon flux than the preferred channel of TRpV ($\tau^-l^+\nu$), which can be checked by comparing the corresponding lines of Fig. (2). Basically, we may conclude that for the given gravitino lifetime, the TRpV scenario generates an enhancement of charged leptons in comparison to BRpV and at the same time the flux of photons is slightly smaller. Mixing these two effects we can see that the TRpV model is able to generate a sizable amount of electrons at a lower photon cost in comparison to BRpV, which can be seen in Fig. (3). In the following sections we study the TRpV model considering the data from AMS-02 [2–4], CALET [5], DAMPE [6] and Fermi-LAT [7] in order to check this scenario with current data and a proper statistical analysis.

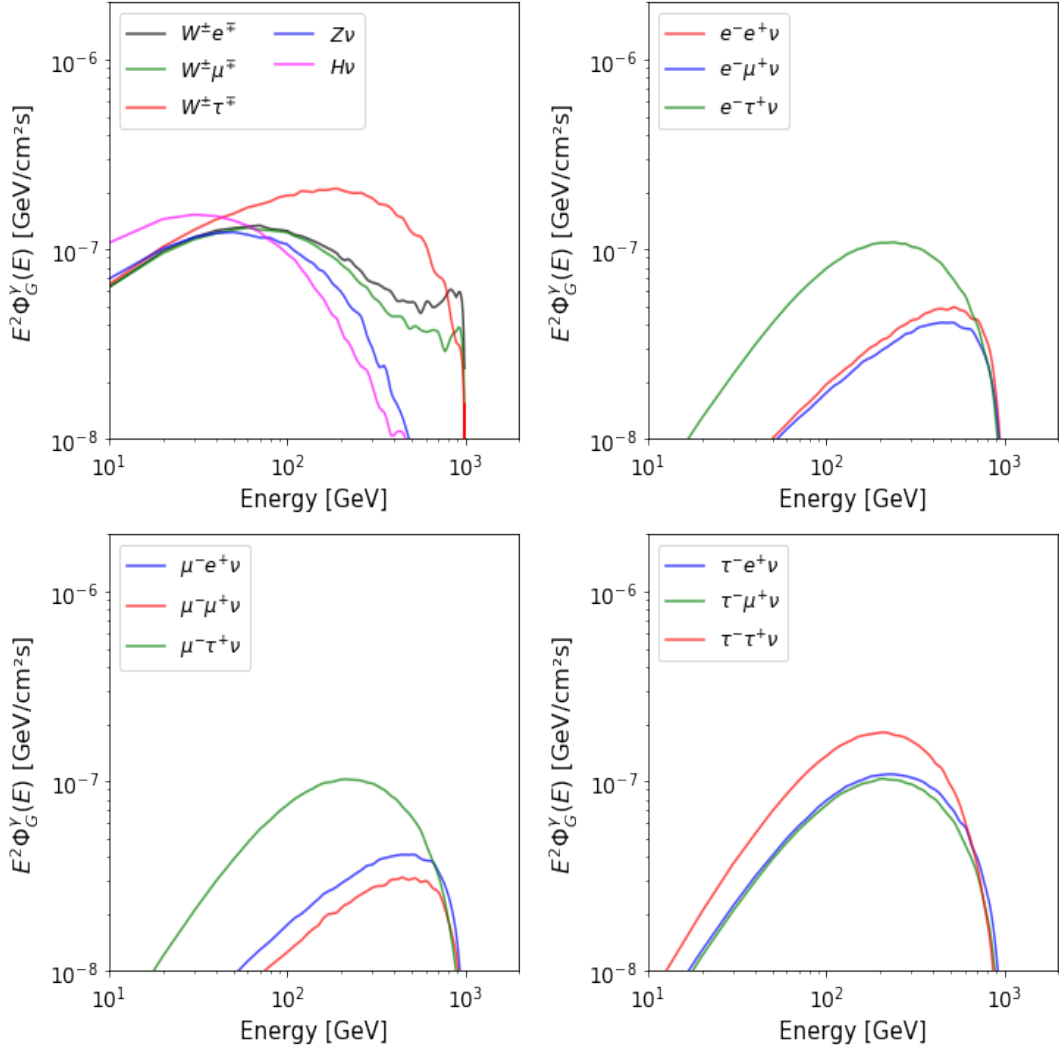


Figure 2. Photon spectrum for bilinear and trilinear models. The bilinear case is shown in the top left panel. The trilinear cases are given by the top right panel, which includes the channels 1, 2 and 3, the bottom left panel, which includes the channels 4, 5 and 6, and the bottom right panel, which includes the channels 7, 8 and 9 (see definitions of these channels in the main text). The gravitino lifetime is the same and equal to $\tau_G = 10^{26} s$ in both panels.

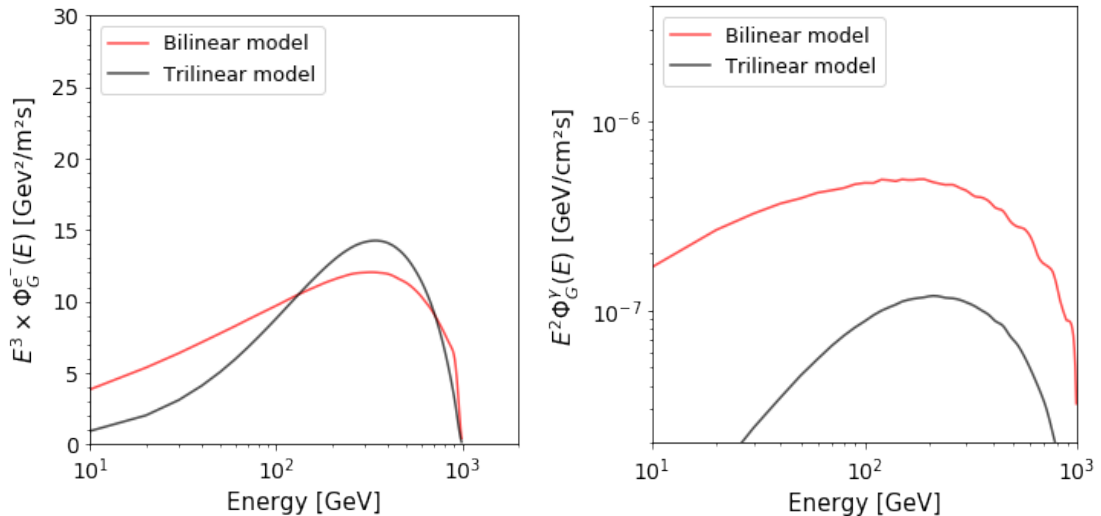


Figure 3. Expected electron (left panel) and photon spectrum (right panel) for bilinear and trilinear models. In bilinear scenario we use $m_G = 2$ TeV, $\tau_G = 1.3 \times 10^{26}$ s and $BR(\psi \rightarrow W^+ \tau^-) = 80\%$, which correspond to one of the preferred scenarios obtained in Ref. [15]. In trilinear case we use $m_G = 2$ TeV, $\tau_G = 3.6 \times 10^{26}$ s and $BR(\psi \rightarrow \tau^- l^+ \nu) = 58\%$, which is one of the best fit scenarios found in this paper.

4 Standard contributions to electron, positron and γ -rays

The standard contribution to the flux of electrons and positrons detected at Earth arise from local galactic sources, such as pulsars or spalls from primary cosmic rays interacting with the interstellar medium. The majority of this flux can be accounted by a diffuse power law spectra [20], which is expected from standard astrophysical models. Therefore, we model this contribution with the following expressions:

$$\Phi_B^e(E) = C_e (E/1 \text{ GeV})^{-\gamma_e} \quad \text{for electrons and} \quad (4.1)$$

$$\Phi_B^p(E) = C_p (E/1 \text{ GeV})^{-\gamma_p} \quad \text{for positrons} \quad (4.2)$$

where the values of C_e, C_p, γ_e and γ_p are obtained from the fit to the data. The astrophysical background term in the electron flux attempt to model primary and secondary production, while in the positron flux equation represents only secondary production. However, in order to accommodate the rise of the positron flux above ≈ 200 GeV, reported by AMS-02 [2], we definitely need something else. In order to cover this gap we include a new source term injecting electrons and positrons at high energies, that arises from the decay of gravitinos into SM particles. The details about this contribution are given in the following section.

The charged SM particles produced from gravitino decays must produce γ -rays, that would reach specialized detectors, such as Fermi-LAT. Indeed, it has been noticed that the DM emission of γ -rays at high galactic latitude ($|b| > 20^\circ$) would be indistinguishable from the overall isotropic gamma-ray background (IGRB) [8], which is a tenuous diffuse component. Since resolved sources are not part of the IGRB, this observable depends on the point source threshold of the specific experiment. Thus, it is preferable to consider the measurement of

the total extra-galactic γ -ray background (EGB), which represents a superposition of all γ -ray sources, both resolved and unresolved, from the edge of the Milky Way to the edge of the observable Universe [7]. In other words, the EGB is the sum of the IGRB plus resolved sources. It turns out that the majority of the EGB can be associated to the emission of standard sources [8]. Therefore, we use the EGB to put limits on DM contributions. The standard contributions to the EGB are taken from [15] and references therein.

5 Gravitino contributions to electron, positron and γ -rays in TRpV

On top of the standard astrophysical background we consider the contribution of gravitino decays. Since different neutrinos are indistinguishable, we must deal with 9 independent channels, i.e. $l_i^- l_j^+ \nu$ for $i, j = e, \mu, \tau$. Therefore the relation between branching fractions and individual trilinear couplings is not necessarily direct. We define the branching fractions from Br_1 to Br_9 , such that $Br_1 = Br(\psi \rightarrow e^- e^+ \nu)$, $Br_2 = Br(\psi \rightarrow e^- \mu^+ \nu)$, etc. Considering these channels we can model the amount of electrons, positrons or γ -rays produced on gravitino decays as:

$$\Phi_G^\eta(E) = \frac{1}{m_G \tau_G} \sum_{j=1}^9 Br_j \frac{dN_j^\eta}{dE} D_{\text{factor}}^\eta, \quad (5.1)$$

where m_G and τ_G are the mass and lifetime of the gravitino respectively. The term $\eta = e, p, \gamma$ when we consider electron, positron or γ -ray flux, correspondingly. The D_{factor}^η is proportional to the density of DM in the case of $\eta = \gamma$, in the other cases is a more complex term that depends on the DM density and the propagation of charged particles in the Galaxy. The term dN_j^η/dE is the amount of electrons, positrons, or γ -rays produced per gravitino decay and energy of the corresponding particle, propagated to the Earth position.

Effective channels for data analysis: electron-positron

For the computation of the electron-positron spectrum at Earth's position, we consider an approach similar to that used in our previous work [15], therefore we suggest to follow that work and references therein, to check the details on the total flux computations, including propagation effects. For simplicity, we restrict the current analysis to the MED propagation working point only.

Now, let's focus on the spectrum of charged leptons. In principle, we can get each branching fraction as a function of the free parameters of the fundamental model, such as the trilinear couplings λ_{ijk} and the mass of super-symmetric scalars. However, for our purposes it is sufficient to consider directly the branching fractions as the effective free parameters for the fit of the electron and positron spectrum. Besides, by considering that some of the channels generate a very similar spectrum (see Fig. 1 right panel), we can reduce the model degrees of freedom further, by grouping decay channels as follows:

$$\Phi_G^e(E) \propto \frac{1}{m_G \tau_G} \left[\alpha_1 \frac{dN_1^e}{dE} + \alpha_2 \frac{dN_2^e}{dE} + \alpha_3 \frac{dN_3^e}{dE} \right], \quad (5.2)$$

where $\alpha_1 = Br_1 + Br_2 + Br_3$, $\alpha_2 = Br_4 + Br_5 + Br_6$ and $\alpha_3 = Br_7 + Br_8 + Br_9$ with $\alpha_1 + \alpha_2 + \alpha_3 = 1$. Thus, we only need to find two independent effective branching fractions in order to adjust the electron spectrum. Analogously, for the positron spectrum we have that

$$\Phi_G^p(E) \propto \frac{1}{m_G \tau_G} \left[\beta_1 \frac{dN_1^p}{dE} + \beta_2 \frac{dN_3^p}{dE} + \beta_3 \frac{dN_3^p}{dE} \right],$$

where $\beta_1 = Br_1 + Br_4 + Br_7$, $\beta_2 = Br_2 + Br_5 + Br_8$ and $\beta_3 = Br_3 + Br_6 + Br_9$. In principle, it seems that we need two extra parameters to fit the positron spectrum, however it is possible to show that electron and positron spectra are indeed equivalent. In order to find this explicitly, we use the equivalence between branching fractions of conjugated decay channels, such that $Br_2 = Br_4$, $Br_3 = Br_7$ and $Br_6 = Br_8$. Thus, we can rewrite the positron spectrum as

$$\Phi_G^p(E) \propto \frac{1}{m_G \tau_G} \left[\alpha_1 \frac{dN_3^p}{dE} + \alpha_2 \frac{dN_5^p}{dE} + \alpha_3 \frac{dN_1^p}{dE} \right]$$

Finally, we can use that the electron spectrum from a given channel must be equal to the positron spectrum of the conjugated one to find that

$$\Phi_G^p(E) \propto \frac{1}{m_G \tau_G} \left[\alpha_1 \frac{dN_1^e}{dE} + \alpha_2 \frac{dN_2^e}{dE} + \alpha_3 \frac{dN_3^e}{dE} \right] \quad (5.3)$$

$$\Phi_G^p(E) = \Phi_G^e(E) \quad (5.4)$$

Therefore, in order to fit the electron-positron data we only need to consider two independent effective branching fractions. Notice that the equivalence between electron and positron spectra is expected from general arguments related to charge conjugation symmetry, here we just wanted to show and verify this issue explicitly in terms of our effective parameters.

Effective channels for data analysis: γ -rays

Analogously to the electron-positron flux, we may discuss the total contribution of gravitino decays to the EGB measured at Earth's position by considering the following expression

$$\Phi_G^\gamma(E) \propto \frac{1}{m_G \tau_G} \sum_{i=1}^9 Br_i \frac{dN_i^\gamma}{dE} \quad (5.5)$$

where Br_i are the same branching fractions that appear in front of the electron-positron spectra. Thus, we can use some results of the previous section in order to manipulate these branching fractions and optimize the contribution of gravitino decays to the EGB.

Indeed, we have seen that the spectrum of charged leptons effectively depends on the parameters α_1 , α_2 and α_3 , which are given by the sum of individual branching fractions. Therefore, after the fit of the electron-positron data, the individual branching fractions are still undetermined. Basically, we are free to choose Br_1 to Br_9 subject to the conditions, $\alpha_1 = Br_1 + Br_2 + Br_3$, $\alpha_2 = Br_4 + Br_5 + Br_6$ and $\alpha_3 = Br_7 + Br_8 + Br_9$. Besides, we also must satisfy that $Br_2 = Br_4$, $Br_3 = Br_7$ and $Br_6 = Br_8$. Considering these conditions and the particular shapes of the γ -ray spectrum in our model (see Fig. 2), it is possible to show that the combination that minimizes the total γ -ray spectrum is given by

$$\begin{aligned} Br_1 &= \alpha_1, & Br_8 &= Br_6 = 0 \\ Br_5 &= \alpha_2, & Br_4 &= Br_2 = 0 \\ Br_9 &= \alpha_3, & Br_7 &= Br_3 = 0 \end{aligned} \quad (5.6)$$

In the following section, we evaluate the contribution of gravitino decays to the electron-positron spectrum and the EGB by using only this combination between branching fractions and effective parameters.

6 Statistical analysis setup

In order to compare the results about the optimization of the TRpV model with those obtained with the analogous BRpV scenario in our previous work [15], we start the statistical analysis of TRpV by considering the same sources of data for electron-positron cosmic rays and γ -rays as in our previous work. This data is composed by the the following sets:

- D_1 : The positron fraction measured by AMS-02 between 0.5 and 500 GeV [2],
- D_2 : The independent measurement of the electron and positron fluxes by AMS-02 between 0.5 and 700 GeV [3],
- D_3 : The measurement of the sum of electron and positron spectrum measured by AMS-02 between 0.5 GeV and 1 TeV [4],
- D_4 : The spectrum of isotropic diffuse gamma-ray emission between 100 MeV and 820 GeV measured by Fermi-LAT [7], from which we derive the limits on the EGB,

Therefore, in the first step of the analysis, we use the first three data sets together in order to adjust the free parameters of the TRpV scenario. The last one is used to cross check the consistency of the best fit model to the EGB limits. Besides, we also consider other sources of data about electron and positron cosmic rays in order to study the consistency of our previous results when more data is considered. These sets are given by:

- D_5 : The extended measurement of the sum of electron and positron spectrum by CALET between 11 GeV and 4.8 TeV [5],
- D_6 : The direct detection of the spectrum of electrons plus positrons measured by DAMPE between 25 GeV and 4.6 TeV [6] and

Thus, in the second step of the statistical analysis, we adjust the parameters of the TRpV scenario considering different combinations between AMS, CALET and DAMPE data and in every case we cross-check the consistency of the optimized models against the EGB limits defined from D_3 .

Likelihood definition and optimization algorithm

Considering the definition of the standard astrophysical sources of electron and positron signals and the analysis of the gravitino sector of the previous section, we identify a total of eight free parameters that need to be optimized in order to adjust the electron and positron data. These parameters are given by C_e , γ_e , C_p , γ_p , m_G , τ_G , α_1 and α_2 . Anyway, we notice that each data set shown above may depend only on a subset of these parameters.

In order to evaluate the goodness of the fit for a given point in this parameter space, we use a set of Gaussian likelihoods. Since the full likelihood function can be quite long and indeed can vary depending on the data sets considered for the analysis, here we only show the part that corresponds to the positron measurements, which is given by

$$\log \mathcal{L}_{\text{Positrons}} = -\frac{1}{2} \sum_i \left(\frac{(\Phi_D^p(E_i) - \Phi_M^p(\theta_p, E_i))^2}{(\sigma_D^2 + j \times (\Phi_D^p(\theta_p, E_i))^2)} - \frac{1}{(\sigma_D^2 + j \times (\Phi_D^p(\theta_p, E_i))^2)} \right), \quad (6.1)$$

with σ_D the statistical uncertainty of the measurement D and $\Phi_D^p(E_i)$ the observed flux of positrons in the data set D . The parameter j increases the nominal uncertainty by a fraction of the model, to account for systematic effects and correlations among different data sets [21]. In this case, the model is defined as

$$\Phi_M^p(\theta_p, E_i) = \Phi_B^p(C_p, \gamma_P, E_i) + \Phi_G^p(m_G, \tau_G, \alpha_1, \alpha_2, E_i). \quad (6.2)$$

The likelihood functions considering other measurements can be defined analogously. In order to explore the full likelihood, find the best fit values and credible regions of our unknown parameters, we use the Bayesian inference package Multinest [22] through its Python interface PyMultinest [23]. Later, we consider the best fit predictions of these scenarios in the γ -ray region in order to check the consistency of our results with EGB limits.

7 Results

In the first step of our statistical analysis we adjust the TRpV parameters by considering the data sets D_1 , D_2 and D_3 , which is the same data used in our previous work. Indeed, we consider two cases, in the first one we use $D_1 + D_2$, such that we consider the AMS-02 measurements of the positron fraction and the independent measurements of electrons and positrons. In the second case, we consider $D_1 + D_2 + D_3$ in order to discuss the effects of considering the sum of electron plus positron, also measured by AMS-02, as an extra source of information. The summary of our results concerning these two cases are given in Table 1 under the columns Case 1 and Case 2 respectively.

From the results of Table 1 we see that in both cases the lifetime of the gravitino is around $4 \times 10^{26} s$ with a strong preference of the channel $\tau^- l^+ \nu$. The best fit lines for Case 1 and 2 for the positron fraction are given in the top panels of Fig. 4. The predictions for the electron plus positron flux in both cases are given in Fig. 5. We notice that both cases produce very similar results, which are almost indistinguishable by simple inspection. In Fig. 6 top panel, we show the comparison between the γ -ray distributions of both cases and the EGB limits, which are obtained as in our previous work. In these plots we can find our main results, since here we can see that the γ -ray spectrum obtained in the TRpV scenario is indeed compatible with EGB limits. The central values of the spectrum just touch the upper limit points and almost half the points inside the 95% C.L. regions are below these limits.

We also notice that the best fit of the gravitino mass can vary from 1.2 to 2.3 TeV when we pass from Case 1 to Case 2. This is probably because the measurement of the electron plus positron signal, included only in Case 2, indeed can reach higher energies than the isolated measurement of electrons and positrons, which in turn may shift the spectrum of gravitino decays to higher energies. Although this effect is not super clear when we compare the figures for Case 1 and Case 2, we will see that this effect is more notorious when we consider the data about electron plus positron from CALET and DAMPE.

Thus, in the second step of the analysis we adjust the TRpV parameters by considering two new sources of the electron plus positron measurements. The first one (Case 3) considers the combination $D_1 + D_2 + D_5$ in order to replace the measurement of AMS-02 by the

Parameter	Case 1	Case 2	Case 3	Case 4
C_p [1/GeV cm ² s str]	14.90	14.74	14.93	14.37
γ_p	3.11	3.10	3.11	3.09
C_e [1/GeV cm ² s str]	426.10	421.77	422.08	422.67
γ_e	3.27	3.27	3.27	3.27
m_G [GeV]	1281	2274	3604	3751
τ_G [10 ²⁶ s]	4.61	3.59	2.27	2.29
$\alpha_1 : e^- l^+ \nu$	0.43	0.06	0.03	0.32
$\alpha_2 : \mu^- l^+ \nu$	0.03	0.36	0.15	0
$\alpha_3 : \tau^- l^+ \nu$	0.54	0.58	0.82	0.68

Table 1. Best fit parameters for the different cases defined in previous section. Recall that $\alpha_3 = 1 - (\alpha_1 + \alpha_2)$ by definition.

analogous measurements of CALET. In the second case (Case 4) we implement a similar approach by considering DAMPE data. The obtained best fit values of these two cases are given in Table 1 under the columns Case 3 and Case 4. We clearly can see that in both cases the best fit gravitino mass suddenly increases from 2 TeV (Case 2) to almost 4 TeV (Cases 3 and 4). The value of the gravitino lifetime decreases from 4×10^{26} s to 2.3×10^{26} s probably in order to balance the change on mass. The preference for the channel $\tau^- l^+ \nu$ is hold it as in previous cases. In Fig. 4 we see the corresponding predictions for the positron fraction, which seem compatible with current data.

In Fig. 5 we see the predictions for electron plus positron for Case 3 and Case 4, where we can see a big change from the initial two cases, which is explained by the big difference within the observed data itself. More importantly and as consequence of the previous results, we see in Fig. 6 bottom panels that these two last cases are in conflict with the EGB limits. Since the discrepancy of our predictions mostly differ because of the difference on the considered data, going from allowed to forbidden scenarios, we believe that further conclusions about the TRpV scenario must consider the study about the origin of the discrepancy in the data about electron plus positron measurements.

8 Conclusions

In this work we consider a dark matter model that includes a meta-stable gravitino that can decay to SM particles only through TRpV couplings. This model is introduced in order to adjust the electron-positron cosmic ray data, in particular the anomalous rising in the positron fraction observed by AMS-02 and others. Based on the comparison between decay configurations allowed in TRpV and BRpV, we suggest that in the former it is possible to adjust the electron-positron data in consistency with EGB limits, thus improving the results obtained only with BRpV decays, that overshoot these limits.

From the statistical analysis of the TRpV scenario, considering the data from AMS-02, CALET, DAMPE and Fermi-LAT, we find two important results. On the one hand, we explicitly show that TRpV is indeed able to explain the electron-positron data measured by AMS-02. More importantly, we obtain that these results are compatible with the EGB limits obtained from Fermi-LAT data. This is an improvement on the results obtained by using only BRpV couplings.

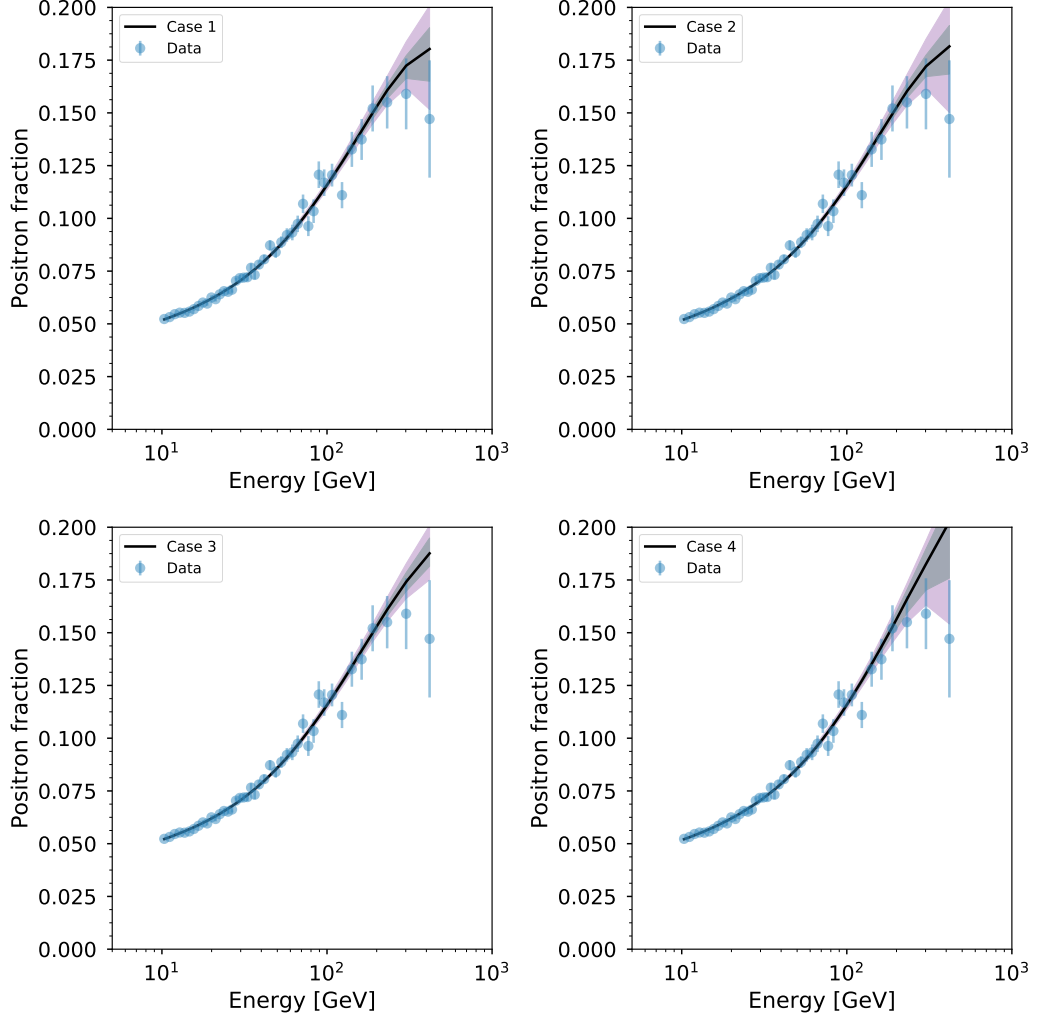


Figure 4. Best fit results for positron fraction. The scenarios from Case 1 to Case 4 are ordered from left to right and from top to bottom.

On the other hand we show that this compatibility with the EGB limits can be affected by the inclusion of electron-positron data from CALET and DAMPE. Basically, the extended domain of the electron plus positron flux measured by these two experiments shifts the gravitino contribution to higher energies, which is the region constrained by the EGB limits. We notice that the root of this conflict is given by the discrepancy between AMS-02 electron plus positron data and the corresponding data from CALET and DAMPE. Finally, we suggest a deeper study about this discrepancy in order to further analyze the gravitino dark matter with TRpV model and indeed any other dark matter scenario with signals in these regions.

Acknowledgments

We acknowledge support from the ANID-Chile grants Basal-CATA PFB-06/2007 and Basal AFB-170002 (J.B.), FONDECYT Postdoctorados 3160439 (J.B.) and the Ministry of Economy, Develop-

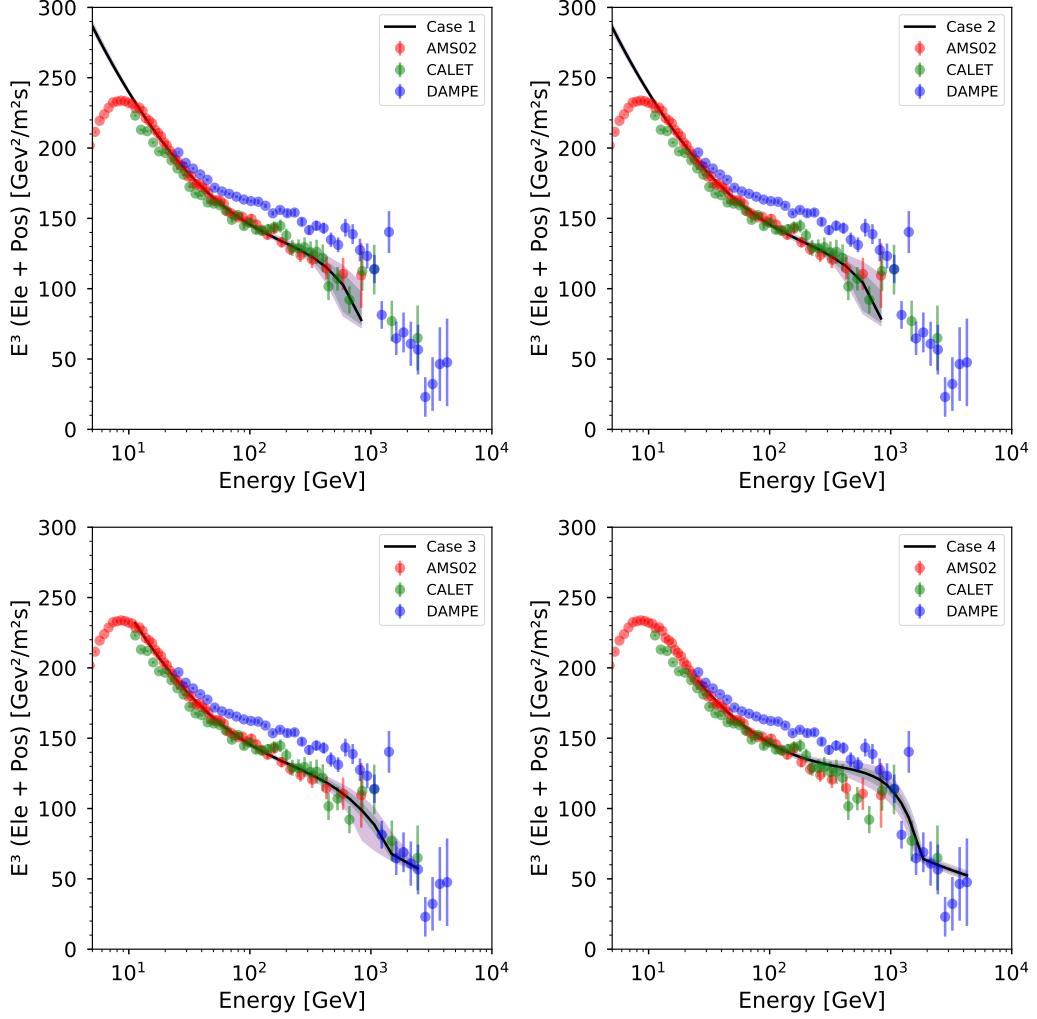


Figure 5. Best fit results for electron plus positron flux. The scenarios from Case 1 to Case 4 are ordered from left to right and from top to bottom.

ment, and Tourism’s Millennium Science Initiative through grant IC120009, awarded to The Millennium Institute of Astrophysics, MAS (J.B.). B.P. is currently supported by a Postdoctoral Fellowship from the joint committee ESO-Government of Chile. B.P. also thanks the support of the State of São Paulo Research Foundation (FAPESP) during the initial stages of this work. E.C. is supported by grant; FONDECYT No. 1190886, N.V. is supported by FONDECYT No. 11170109, E.C. and N.V. are also supported by grant ANID PIA/APOYO AFB180002.

A Appendix: discussion about the gravitino lifetime and neutrino masses

The full expressions for the gravitino decay width, considering trilinear R-Parity violation, are given in [17]. For instance, from these expressions we can get an approximated formula for the leptonic decay $\Gamma(\tilde{G} \rightarrow \nu_i e_j \bar{e}_k)$ by assuming that the mass of the sleptons mediating the three body decay are equal, such that $m_{\tilde{\nu}_{iL}} = m_{\tilde{e}_{jL}} = m_{\tilde{e}_{kR}} = \tilde{m}$, and expand in Taylor series around the variable m_G/\tilde{m} to obtain

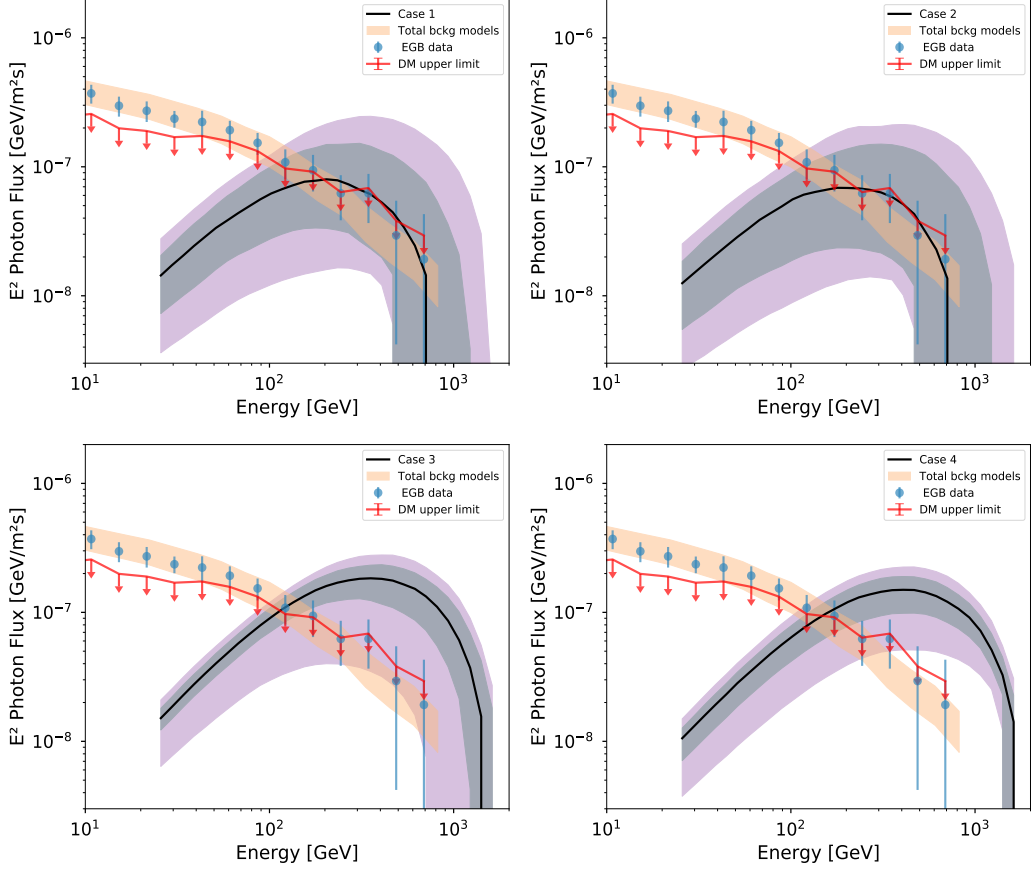


Figure 6. Best fit results for photon flux compared to EGB limits. The scenarios from Case 1 to Case 4 are ordered from left to right and from top to bottom.

$$\Gamma(\tilde{G} \rightarrow \nu_i e_j \bar{e}_k) \approx \frac{1}{96(2\pi)^3} \frac{\lambda_{ijk}^2}{8M_\star^2} \frac{m_G^7}{\tilde{m}^4}, \quad (\text{A.1})$$

This result shows that the decay width (lifetime) decreases (increases) rapidly as we increase \tilde{m} , as expected. We expect that a similar behavior should be obtained even when the mass of sleptons are not equal. Indeed, we have verified this expectation numerically, by evaluating the full expression given in [17] using the maximum numerical precision in Mathematica. For instance, in Fig. 7 we plot the gravitino lifetime as a function of $m_{\tilde{\nu}_{iL}}$ for $m_{\tilde{e}_{jL}} = m_{\tilde{\nu}_{iL}}/2$ and $m_{\tilde{e}_{kR}} = m_{\tilde{\nu}_{iL}}/5$. Also, in the same figure we plot the lifetime derived from Eq. A.1 evaluated at $\tilde{m} = m_{\tilde{\nu}_{iL}}/2$ in order to check that both approaches, exact computation and approximated formula, behave similarly. Therefore, the gravitino lifetime can be written as in Eq. A.2,

$$\tau_G \approx 10^{26} \text{ s} \left(\frac{1}{\lambda_{ijk} \lambda_{ijk}} \right) \left(\frac{\tilde{m}}{2 \times 10^7 \text{ GeV}} \right)^4 \left(\frac{1 \text{ TeV}}{m_G} \right)^7 \quad (\text{A.2})$$

where we have normalized with respect to 10^{26} s since this is the order of magnitude required

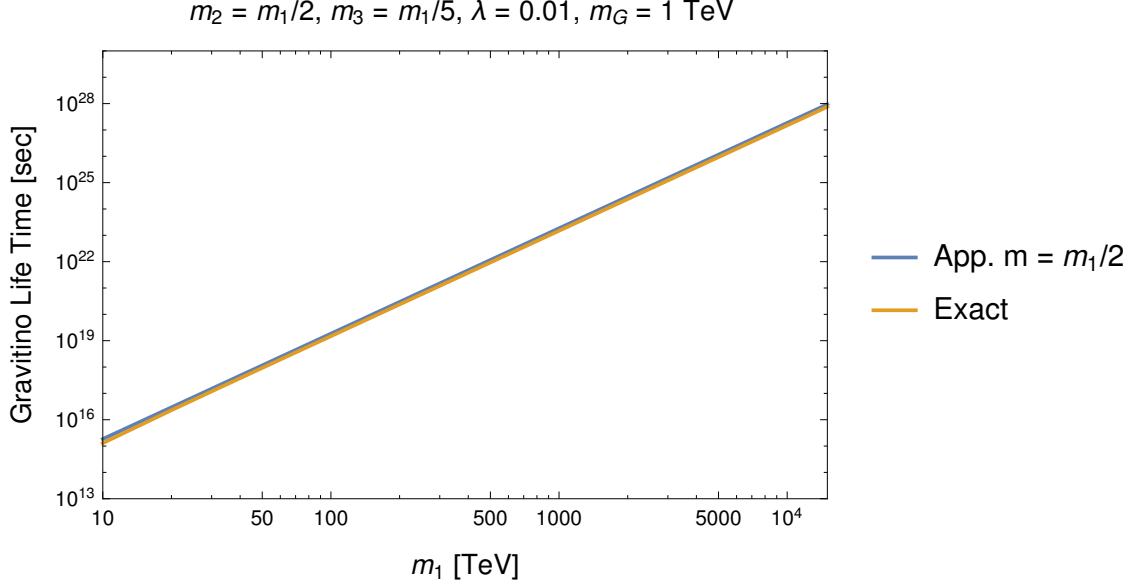


Figure 7. Gravitino life time in Trilinear RpV for $\lambda_{ijk} = 0.01$, $m_G = 1 \text{ TeV}$. For simplicity we use m_1, m_2, m_3 and m instead of $m_{\tilde{\nu}_{iL}}, m_{\tilde{e}_{jL}}, m_{\tilde{e}_{kR}}$ and \tilde{m} .

by experiments such as AMS-02 and Fermi-LAT in order to fit the electron positron data in the first case or to avoid gamma ray constraints in the second.

In TRpV the neutrino mass matrix receives contributions from 1-loop diagrams that contain both a charged lepton and the corresponding slepton. Indeed, we have derived the following expression

$$M_{ij}^{\nu(1)} \approx \frac{1}{16\pi^2} \sum_{gr} s_{\tilde{l}} c_{\tilde{l}} (\lambda_{igr} \lambda_{jrg} + \lambda_{jgr} \lambda_{irg}) m_g \ln \frac{m_{\tilde{l}_{r2}}^2}{m_{\tilde{l}_{r1}}^2}$$

where i and j are neutrino generation indices that runs from 1 to 3. g is a charged lepton index that also run from 1 to 3, as well as r which is a slepton index. Thus, it can be seen that for order one parameters, $s_{\tilde{l}} \sim c_{\tilde{l}} \sim \ln(m_{\tilde{l}_{r2}}^2/m_{\tilde{l}_{r1}}^2) \sim 1$, we can get neutrino masses around the eV scale for $\lambda_{ijk} \approx 0.01$ even for $m_g \approx m_e$. Indeed, by following the expressions given in [18] for the contribution of λ' trilinear terms, we can get by analogy that the dominant term in the leptonic sector is

$$\begin{aligned} M_{ij}^{\nu(1)} &\approx \frac{1}{8\pi^2} \lambda_{i23} \lambda_{j32} \frac{m_\mu m_\tau A_\tau}{\tilde{m}^2} \\ &\approx 2 \times 10^{-2} \text{eV} \lambda_{i23} \lambda_{j32} \left(\frac{10^8 \text{ GeV}}{\tilde{m}} \right) \\ &\approx 2 \times 10^{-2} \text{eV} (\lambda_{i23} \lambda_{j32})^{1/4} \left(\frac{\tau_G}{10^{26} \text{ s}} \right)^{1/4} \left(\frac{m_G}{2 \text{ TeV}} \right)^{7/4} \end{aligned}$$

where A_τ is a free parameter that can be considered of order \tilde{m} , as it is done in [18]. Thus, if we consider this formula together with Eq. (A.2) we see that we can have contributions to the neutrino mass matrix of order 10^{-2} eV for trilinear couplings of order one, scalar mass scale around 10^8 GeV and $\tau_G \approx 10^{26} \text{ s}$.

B Complementary results from the fit

In this section we show the complementary plots about electron and positron spectra concerning the statistical analysis of Cases 1 to 4, which are detailed in the main text.

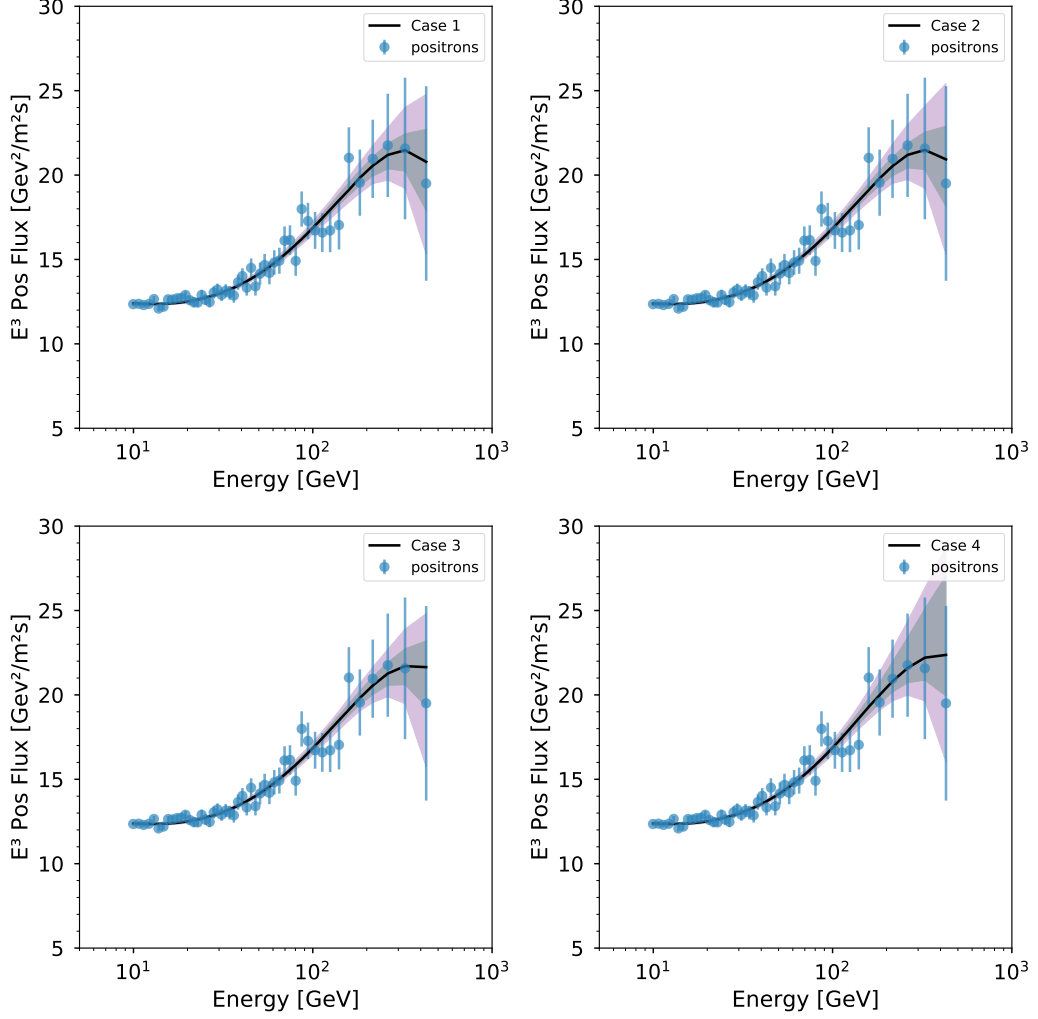


Figure 8. Best fit results for positron flux. The scenarios from Case 1 to Case 4 are ordered from left to right and from top to bottom.

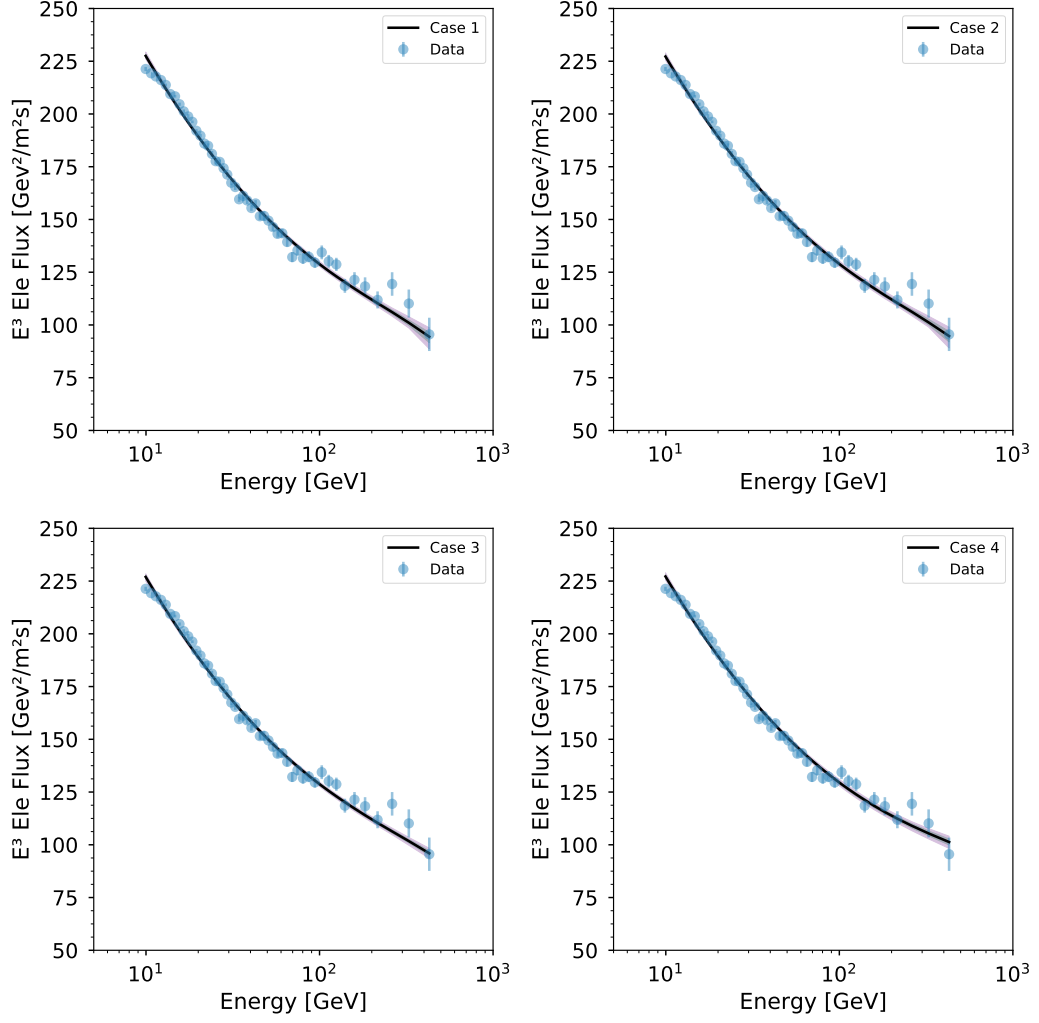


Figure 9. Best fit results for electron flux. The scenarios from Case 1 to Case 4 are ordered from left to right and from top to bottom.

References

- [1] **PAMELA** Collaboration, O. Adriani et al., *An anomalous positron abundance in cosmic rays with energies 1.5-100 GeV*, *Nature* **458** (2009) 607–609, [[arXiv:0810.4995](#)].
- [2] **AMS** Collaboration, L. Accardo et al., *High Statistics Measurement of the Positron Fraction in Primary Cosmic Rays of 0.5500 GeV with the Alpha Magnetic Spectrometer on the International Space Station*, *Phys. Rev. Lett.* **113** (2014) 121101.
- [3] **AMS** Collaboration, M. Aguilar et al., *Electron and Positron Fluxes in Primary Cosmic Rays Measured with the Alpha Magnetic Spectrometer on the International Space Station*, *Phys. Rev. Lett.* **113** (2014) 121102.
- [4] **AMS** Collaboration, M. Aguilar et al., *Precision Measurement of the $(e^+ + e^-)$ Flux in Primary Cosmic Rays from 0.5 GeV to 1 TeV with the Alpha Magnetic Spectrometer on the International Space Station*, *Phys. Rev. Lett.* **113** (2014) 221102.
- [5] O. Adriani et al., *Extended Measurement of the Cosmic-Ray Electron and Positron Spectrum from 11 GeV to 4.8 TeV with the Calorimetric Electron Telescope on the International Space Station*, *Phys. Rev. Lett.* **120** (2018), no. 26 261102, [[arXiv:1806.0972](#)].
- [6] **DAMPE** Collaboration, G. Ambrosi et al., *Direct detection of a break in the teraelectronvolt cosmic-ray spectrum of electrons and positrons*, *Nature* **552** (2017) 63–66, [[arXiv:1711.1098](#)].
- [7] **Fermi-LAT** Collaboration, M. Ackermann et al., *The spectrum of isotropic diffuse gamma-ray emission between 100 MeV and 820 GeV*, *Astrophys. J.* **799** (2015) 86, [[arXiv:1410.3696](#)].
- [8] D. Hooper, *TASI Lectures on Indirect Searches For Dark Matter*, [[arXiv:1812.0202](#)].
- [9] M. Grefe, *Neutrino signals from gravitino dark matter with broken R-parity*, [[arXiv:1111.6041](#)].
- [10] M. Cirelli, E. Moulin, P. Panci, P. D. Serpico, and A. Viana, *Gamma ray constraints on decaying dark matter*, *Phys. Rev. D* **86** (Oct., 2012) 083506, [[arXiv:1205.5283](#)].
- [11] S. Ando and K. Ishiwata, *Constraints on decaying dark matter from the extragalactic gamma-ray background*, *JCAP* **1505** (2015), no. 05 024, [[arXiv:1502.0200](#)].
- [12] M. Laletin, *A no-go theorem for the dark matter interpretation of the positron anomaly*, *Frascati Phys. Ser.* **63** (2016) 7–12, [[arXiv:1607.0204](#)].
- [13] W. Liu, X.-J. Bi, S.-J. Lin, and P.-F. Yin, *Constraints on dark matter annihilation and decay from the isotropic gamma-ray background*, *Chin. Phys.* **C41** (2017), no. 4 045104, [[arXiv:1602.0101](#)].
- [14] K. Belotsky, R. Budaev, A. Kirillov, and M. Laletin, *Fermi-LAT kills dark matter interpretations of AMS-02 data. Or not?*, *JCAP* **1701** (2017), no. 01 021, [[arXiv:1606.0127](#)].
- [15] E. Carquin, M. A. Diaz, G. A. Gomez-Vargas, B. Panes, and N. Viaux, *Confronting recent AMS-02 positron fraction and Fermi-LAT extragalactic γ -ray background measurements with gravitino dark matter*, *Phys. Dark Univ.* **11** (2016) 1–10, [[arXiv:1501.0593](#)].
- [16] M. Grefe, *Unstable Gravitino Dark Matter - Prospects for Indirect and Direct Detection*, [[arXiv:1111.6779](#)].
- [17] G. Moreau and M. Chemtob, *R-parity violation and the cosmological gravitino problem*, *Phys.Rev.* **D65** (2002) 024033, [[hep-ph/0107286](#)].
- [18] E. J. Chun and S. C. Park, *Neutrino mass from R-parity violation in split supersymmetry*, *JHEP* **01** (2005) 009, [[hep-ph/0410242](#)].
- [19] G. Giudice and A. Romanino, *Erratum to: Split supersymmetry [nucl. phys. b 699 (2004) 65]*, *Nuclear Physics B* **706** (Jan, 2005) 487.

- [20] **AMS Collaboration** Collaboration, M. Aguilar et al., *First Result from the Alpha Magnetic Spectrometer on the International Space Station: Precision Measurement of the Positron Fraction in Primary Cosmic Rays of 0.5-350 GeV*, *Phys.Rev.Lett.* **110** (2013) 141102.
- [21] D. W. Hogg, J. Bovy, and D. Lang, *Data analysis recipes: Fitting a model to data*, 2010.
- [22] F. Feroz, M. Hobson, and M. Bridges, *Multinest: an efficient and robust bayesian inference tool for cosmology and particle physics*, *Mon. Not. Roy. Astron. Soc.* **398** (2009) 1601–1614, [[arXiv:0809.3437](#)].
- [23] J. Buchner, A. Georgakakis, K. Nandra, L. Hsu, C. Rangel, M. Brightman, A. Merloni, M. Salvato, J. Donley, and D. Kocevski, *X-ray spectral modelling of the AGN obscuring region in the CDFS: Bayesian model selection and catalogue*, *Astron. Astrophys.* **564** (2014) A125, [[arXiv:1402.0004](#)].